Comparison of Tensile Fatigue Resistance and Constant Life Diagrams for Several Potential Wind Turbine Blade Laminates

Daniel D. Samborsky*, Timothy J. Wilson†, and John F, Mandell‡
Department of Chemical and Biological Engineering, Montana State University, Bozeman, MT, 59717, USA

Abstract

New fatigue test results are presented for four multidirectional laminates of current and potential interest for wind turbine blades, representing three types of fibers: E-glass, WindStrand™ glass, and carbon, all with epoxy resins. A broad range of loading conditions are included for two of the laminates, with the results represented as mean and 95/95 confidence level constant life diagrams. The constant life diagrams are then used to predict the performance under spectrum fatigue loading relative to an earlier material. Comparisons of the materials show significant improvements under tensile fatigue loading for carbon, WindStrand, and one of the E-glass fabrics relative to many E-glass laminates in the 0.5 to 0.6 fiber volume fraction range. The carbon fiber dominated laminate shows superior fatigue and static strengths, as well as stiffness, for all loading conditions.

Introduction

The fatigue of composite laminates appropriate for wind turbine blades has been the topic of research studies for more than two decades. The findings of these studies are summarized in recent reports [1, 2], and in two current databases [3, 4]. Various models and methodologies for representing fatigue behavior, and using the models and data to predict lifetime under blade spectrum fatigue loads have been developed [2, 5]. An extensive review of the literature in this area has been provided by Nijssen [2]. This paper reports on a large body of new data, comparing

*Research Engineer, † Graduate Student, ‡ Professor

infused and prepreg epoxy matrix laminates with different fibers and fabrics of current interest, under a broad range of loading conditions.

Most utility scale wind turbine blades are currently thought to use E-glass based prepreg or resin infused laminates in a variety of fabrics, with a fiber content in the range of 50% by volume. Basic materials considerations focus on the elastic modulus and tensile fatigue resistance, which are both of concern with E-glass. The tensile fatigue resistance is also known to be sensitive to fiber content and fabric architecture [1]. This study has developed baseline data for several infused E-glass/epoxy laminates with fabrics of current interest, as well as laminates based on WindStrand^{TM} glass fibers and carbon fibers. Fatigue results in the transverse direction of the laminate are also presented for two of the materials.

Constant amplitude fatigue data for a variety of loading conditions are fit to a power law model, then represented on a constant life diagram (CLD) for use in spectrum loading predictions. The data requirements for CLD's of adequate detail for the prediction of spectrum loading lifetime have been of concern in recent literature [2, 5]. Studies by both Nijssen [2] and Sutherland and Mandell [5] have concluded that an important requirement in predicting spectrum loading lifetime is the detail level of the CLD. Sutherland and Mandell [5] explored these effects for two instrumented turbines, as well as the European WISPERX spectrum. Baseline results were determined using the very detailed CLD in Figure 1 which includes thirteen constant amplitude S-N diagrams at different R-values (R is the ratio of minimum to maximum load in a fatigue cycle) for an early glass/polyester laminate, Material DD16 in the DOE/MSU database [3]. Results showed that predictions using a non-linear damage model became consistent when at least five carefully selected R-values concentrated between -2 and 0.5 were used to construct the CLD. R-values close to reversed loading accounted for much of the damage in most loading situations (edge vs. flap, tension or compression side); the CLD in this range is particularly sensitive to changes in mean stress or R due to the transition from tension to compression dominated failure, which is associated with a major change in fatigue resistance for fiberglass laminates. Nijssen, using results from the European OPTIMAT Program [2, 4] reached similar conclusions as to the number of R-curves required. Following these recommendations for R-values, the current paper compares CLD's for the axial and transverse directions of an E-glass based laminate and a hybrid laminate with carbon 0^o plies. A comparison is also given for the performance of these laminates under spectrum loading conditions.

Experimental Methods and Data Reduction

Materials and Processing

Results from four new laminates are presented in this paper, with comparisons to two heavily tested laminates from the two databases, materials DD16 [3] and MD2 [4] (material designations such as DD16 follow the respective database). The following is a description of the materials:

1. DD16. This is an early E-glass/polyester material taken from the DOE/MSU Database [3].
   Lay-up and % 0^o-material: [90/0/±45/0]s; 53%-0^o
   Fiber volume fraction: 0.36
   Fiber and matrix: E-glass and polyester (Corezyn 63-AX-051 with 1% MEKP)
   Fabrics (90, 0, and ±45): D155, D155 and DB120 (Owens Corning Fabrics)
   Process, cure and post-cure temperatures: VARTM, RT, 2 hours at 65^oC
   Laminate fabricated by: MSU

2. MD2. This is a material reported under the European OPTIMAT Program [2, 4]
   Lay-up and % 0^o-material: $[(\pm 45/0)_4 \pm 45]$, 55%-0^o
   Fiber volume fraction: 0.54
   Fiber and matrix: E-glass and epoxy (SP Systems Prime 20, slow hardener)
   Fabrics (0 and ±45): 1250 g/m^2 uni-roving and 810 g/m^2 biaxial (both PPG 2002 roving)
   Process, cure and post-cure temperatures: VARTM, RT, 80^oC
   Laminate fabricated by: OPTIMAT Program

3. QQ1. E-glass/epoxy laminate based on Saertex fabrics
   Lay-up and % 0^o-material: $[\pm 45/0_2]_S$, 64%-0^o
   Fiber volume fraction: 0.53
   Fiber and matrix: E-glass and epoxy (Huntsman/Vantico TDT 177-155)
   Fabrics: (0 and ±45): U14EU920-00940-T1300 (940 g/m^2) and VU-90079-00830-1270
   Process, cure, and post-cure temperatures: VARTM, RT, 6 hours at 70^oC
   Laminate fabricated by: MSU

4. P2B. Hybrid laminate with carbon 0's and glass ±45's; epoxy matrix
   Lay-up and % 0^o-material: $[\pm 45/0_4]$s, 85%-0^o (by volume)
   Fiber volume fraction: 0.55
   Fiber and matrix: carbon, G300 (Mitsubishi); E-glass; epoxy (Newport NCT 307-D1)
   Prepregs (0 and ±45): NCT-307-D1-34-600 and NB-307-D1-7781 497A (0/90 cut at ±45)
   Process and cure temperature: net resin, vacuum bag, 3 hours at 121^oC
   Laminate fabricated by: MSU (prepreg supplied by Newport Adhesives and Composites)

5. SN5-0291. Infused E-glass/epoxy with Vectorply 0^o fabric
   Lay-up and % 0^o material: [±45/0/±45/0/±45], 66% 0^o
   Fiber volume fraction: 0.55
   Fiber and matrix: E-glass and epoxy (Huntsman Araldite LY1564/hardener XB3485)
   Fabrics(0 and ±45): E-LT-5500 (1829 g/m^2,Vectorply) and DBM 1708 (Owens Corning Fabrics)
   Process, cure and post-cure temperature: VARTM, 60^oC and 82^oC
   Laminate fabricated by: TPI (Supplied by Global Energy Concepts/BSDS Program)

6. WS1. WindStrand™ glass fiber laminate
   Lay-up and %-0^o material: [±45/0/±45], 50%-0^o
   Fiber volume fraction: 0.61
   Fiber and matrix: WindStrand™ (HiPER-tex®) and epoxy (MGS L135i/137i hardener)
   Fabrics (0 and ±45): WindStrand™ 17-1200 SE2350M2 (dry strands, 2000 g/m^2) and
   DB 1000 (same strands)

Process, cure and post-cure temperatures: vacuum infusion, 35°C, 90°C
Laminate fabricated by: Owens Corning

Test Methods

Test methods under the OPTIMAT program (material MD2) have been described in detail by Nijssen [2]. Other materials were tested at MSU using methodologies described in more detail elsewhere [1, 6]. Two test specimen geometries were used extensively, shown in Figure 2; the test geometry is defined in the text for each data set. The DB geometry provided consistent gage-section failures under tensile loading, Figure 3. The rectangular geometry was necessary for R-values containing compressive stresses, but fatigue failures occurred most commonly at the edge of the grips or inside the grips (Figure 3). Specimens of both geometries were tested both with and without additional tab material in the grip area, but the tabs had little effect on strength or lifetime at various R-values. Tests reported here did not include additional tab material except for material QQ1 at R = 0.1. All testing used servo-hydraulic machines of various capacity, with hydraulic grips having lateral constraint [1, 6]. The problem of grip failures with stronger laminates like those in this study is an ongoing issue; similar effects were also reported for the OPTIMAT program by Nijssen [2]. Grip failures were relatively unusual in the testing of earlier vintage, lower fiber content materials like DD16 (Figure 1) [1, 7].

Static tests were run under displacement controlled ramp loading, either at a similar rate to the fatigue tests (13 mm/s) or at a slower rate typical of ASTM test standards. The rate can have a significant effect on static strength for glass fiber materials as described later. Fatigue tests were run under sine-wave, load control, constant amplitude. Figure 4 defines the loading conditions for typical R-values. The frequency was varied approximately inversely with maximum load to maintain a constant load rate; individual test frequencies are given in the DOE/MSU database [3], which will be updated for all materials in this study in early 2007. Frequencies were in the 1-10 Hz range to avoid significant heating; surface temperatures were monitored for selected tests, and fatigue specimens were surface cooled with fans [1, 6]. Failure in all cases was taken as complete separation of the test coupon, although significant matrix cracking in the ±45 plies was readily observable well before failure, often on the first fatigue cycle (Fig. 3).

Where fatigue strains are given they are either calculated through the tensile modulus, or, for DB specimens, measured on the first few cycles of the test, using an extensometer. All compressive strains were calculated through the tensile modulus due to the short gage section. In either case the strains are only representative of the first few cycles, and increase gradually as damage accumulates under controlled stress [1, 6].

Fatigue Models and Data Reduction

Data reduction for fatigue tests includes least squares fitting of the fatigue trends with a power law model illustrated for a material DD16 dataset in Figure 5, which compares the power law fit to exponential and three-parameter models. The power law provided a better fit to the fatigue data than the exponential model in all cases [8]. The exponential model tends to better fit the low cycle and static data as shown, but the power law provides a better fit to the higher cycle data, and has also been shown to represent small glass strand data to 10^{10} cycles [6]. The three-parameter model shown provides an improved fit to the overall dataset, and was used to develop the constant life diagram (CLD) in Figure 1 (including a force fit to the power law model stress at very high cycles) [9]. However, the three-parameter model does not provide a consistent set of fitting parameters compared to the power law, and is inconvenient to manipulate. The results in this study used a power law fit to the mean data along with a static mean strength cut-off at low cycles, to preclude predicted stresses above the static strength on the CLD (either static compressive or tensile strength, depending on R-value). The power law model, Eq. [1], was fit to all of the fatigue data except where visual inspection indicated a more representative fit if either low cycle data were excluded or static data were included [8]. These exceptions are indicated where relevant.

$$S(N) = A \cdot N^{B} \tag{1}$$

A statistical treatment to establish 95/95 confidence limits [1, 2] has been carried out for the more complete datasets for materials QQ1 and P2B. In an effort to reduce the range over which extrapolation of data is required (particularly for less steep S-N datasets), the confidence limits were established on the log stress (or log strain) relative to the mean power law fit; the mean fit was obtained from a linear fit to a log stress-log cycles plot following Echtermeyer et al. [10], rather than to log cycles, as is more conventional, since log N is the dependant variable [1, 2]. Equation [2] gives the mean fit on a log stress-log cycles plot

$$\log_{10}\left(S(N)\right) = m \cdot \log_{10}\left(N\right) + b \tag{2}$$

The standard deviation is then determined from individual data points, log S_i and log N_i as:

$$SD = \sqrt{\frac{1}{n-1}\sum_{i=1}^{n}\left(\log_{10}\left(S_i\right) - m \cdot \log_{10}\left(N_i\right) + b\right)^2} \tag{3}$$

Using the one sided tolerance limit multiplier, $c_{1-\alpha,\gamma}$, where the confidence level is 1-α and the probability of survival is γ, the tolerance limit is [1, 2]:

$$S_{CL}(N) = 10^{\left(\log_{10}(N)+b-c_{1-\alpha,\gamma}\cdot SD\right)} \quad (4)$$

In the results, the intercept, b, in Eq. [2], and the term $c_{1-\alpha,\gamma} \cdot SD$ in Eq. [4] are combined into a term "b-tol" resulting in:

$$S_{CL}(N) = 10^{\left(\log_{10}(N)+b-tol\right)} \quad (5)$$

The same procedure is used to find the confidence limit for the static strengths. Figure 6 shows typical mean and 95/95 fits to a material DD16 dataset.

The construction of the CLD from the fatigue models at different R-values has been described in detail by Nijssen [2]. The CLD's involve extrapolation to higher cycles than represented by actual data, using the fatigue models. Simple extrapolation of the 95/95 tolerance limit was used here, but a more rigorous treatment would consider distance from the data points, as discussed by Nijssen [2]. The tolerance limit based on log (stress) implies consideration of the stress variability for a defined lifetime, say 20 years for a blade. A consistent approach has been used in predicting the load scale factors on the WISPERX spectrum to produce a lifetime defined by a particular number of passes through the spectrum.

Results and Discussion

Static Properties

Laminate elastic modulus and ultimate strengths are listed in Table 1. Since the laminates include differing contents of 0^o, 90^o, and $\pm 45^o$ material, the elastic modulus in the longitudinal direction of the 0^o plies, E_L, is also included (taken from unidirectional laminates, adjusted proportionately to 53% fiber; actual unidirectional laminates varied from 53 to 57%). Tensile strength values are compared in Table 2 (determined with DB specimens except for P2B, which used rectangular specimens) for both standard displacement rates, 0.02 mm/s, and also at a faster rate, 13 mm/s, representative of the displacement rate in fatigue. This approximately three orders of magnitude rate difference produces up to 20% strength difference for the glass laminates; rate effects are small for carbon. Rate effects on static strength values should be considered carefully in using results such as S-N datasets and constant life diagrams. For example, while static data at the faster rate are generally used with these datasets in this study and in the DOE/MSU database [3], the slower, standard static strength testing rate is used in the OPTIMAT program [2].

Compression tests used the rectangular specimen geometry with a gage length of 13 mm. Modulus values were determined in tension using slow load steps, over a strain range of 0.1 to 0.3%, with rectangular or BD specimens.

Glass fiber blade designs are often driven in part by deflection limits, so the modulus values are important. The different laminates, described earlier in detail, differ in the lay-up and 0^o ply content. The longitudinal modulus of the 0^o plies gives a more direct basis for comparison. The modulus values in Table 1 demonstrate the importance of higher fiber content (DD16 vs. QQ1 and SN5-0291). The great advantage of carbon fiber 0^o plies in material P2B is also demonstrated in this Table, as is the improved longitudinal modulus of the WS1, with WindStrand™ glass fibers.

Table 1. Static Strength and Modulus Results ; Mean Values with 95/95 Values in Parenthesis (Strengths Determined at the Fatigue Rate, 13 mm/s).

Material and Direction	Tensile Strength (MPa)	Compressive Strength (MPa)	Ultimate Strains (Tensile / Compressive) %	Elastic Modulus (GPa)	0^O Ply Modulus, E_L (GPa)
DD16 (Axial)	632 (539)	-402 (-358)	2.9 / -2.3	18.3	----
QQ1 (Axial)	869 (758)	-690 (-596)	2.6 / -2.1	33.0	42.5
QQ1T (Transverse)	149 (128)	-274 (-233)	0.87 / -2.1	17.0	---
P2B (Axial)	1546 (1301)	-1070 (-914)	1.4 / -1.0	101	123
P2BT (Transverse)	79.4 (72.0)	-240 (-219)	0.89 / -2.6	8.85	---
SN5-0291 (Axial)	837 (605)	----	3.0 / --	29.4	41.6
WS1 (Axial)	865 (692)	---	2.7 / --	32.6	48.3

Table 2. Comparison of Mean Strengths at Standard Static and Fatigue Displacement Rates in the Axial Direction.

Material	Tensile Strength 13 mm/s (MPa)	Tensile Strength 0.02 mm/s (MPa)	% Difference
QQ1	869	691	-21
DD16	632	549	-13
WS1	865	754	-13
SN5-0291	837	732	-13
P2B	1546	1516	-2

Fatigue Results

The various materials were tested under fatigue loading at the R-values given, and the results were fit to Eq. [1] to obtain the mean fit parameters A and B. Equations [2] and [5] were then used to obtain the 95/95 parameters m and

b-tol. Figures 7 (a-c) give fatigue test results and mean and 95/95 fits for E-glass laminate QQ1 and carbon hybrid P2B at three R-values. The mean and 95/95 fits are extrapolated over the entire cycles range shown, but this is not rigorous outside the range of the data used in the fits, as discussed earlier. Table 3 gives fit parameters for all materials and all R-values, except for MD2 which was reported by Nijssen [2], and follows different procedures.

Tensile Fatigue Comparison

Tensile fatigue resistance can be a second design driver in glass fiber blades, in addition to stiffness; as discussed later, this is unlikely to be true in carbon fiber dominated blades due to their much improved tensile fatigue resistance. Figures 8-10 compare the tensile fatigue resistance at R = 0.1 for three glass fiber/epoxy laminates of current interest for blades, having a similar fiber content range (53-61% fiber by volume), QQ1, SN5-0291, and WS1. The first two are E-glass fiber based, the third is based on WindStrand glass fibers. As was the case with the modulus comparison, the three laminates have differing contents of 0^o plies relative to $\pm 45^o$ plies, given earlier, which makes direct comparison in fatigue difficult. Figure 10 compares the materials in terms of the laminate maximum fatigue strain (Figure 9) multiplied by the 0^o ply longitudinal modulus, E_L (Table 1); this is a measure of the maximum 0^o ply stress during fatigue cycling (in the absence of matrix damage), eliminating the effects of the $\pm 45^o$ plies (which contribute little to the axial strength or fatigue resistance [1]). The fatigue test specimens used to obtain the data in Figures 8-10 all were DB geometry and failed in the gage section (Figure 3).

Many earlier infused materials in this relatively high fiber content range showed poor tensile fatigue resistance in terms of the S-N data steepness and the maximum strain which could be withstood for cycles in the 10^6 range [1, 3, 6]. Material QQ1 is typical of many laminates, based on a variety of E-glass fabrics and different resins, which show poor tensile fatigue resistance in this fiber content range. Considering the strain values around 10^6 cycles in Figure 9, the E-glass based SN5-0291 and the WindStrand, WS1, can withstand about twice the maximum strain as can QQ1, a very significant improvement. The 0^o plies in the two superior materials are relatively thick compared with those in QQ1, and the WindStrand fiber is also different (these two datasets are currently being completed for higher cycles). By way of comparison, the MD2 (E-glass) used in the OPTIMAT program shows slightly lower fatigue strains than SN5-0291 at similar cycles [2], with some differences in test methods. Material DD16, E-glass/polyester with a lower fiber content, showed strain levels similar to SN5-0291; however, laminates of similar construction to DD16 transitioned to slightly lower strains than QQ1 at comparable cycles for fiber contents in the 50% range [1, 6].

Table 3: Fatigue Fit Parameters for Various Materials.

Material	R Value	Static Failure Mode	Mean Fit Parameters		95/95 Fit Parameters	
			A	B	m	b-tol
DD16 (Axial)	1.1	Compression	N/A	N/A	N/A	N/A
	1.43	Compression	420.8	-0.0182	-0.0182	2.589
	2	Compression	458.2	-0.0372	-0.0372	2.576
	10	Compression	397.7	-0.0460	-0.0460	2.556
	-2	Compression	648.4	-0.0876	-0.0876	2.772
	-1	Compression	691.1	-0.1280	-0.1280	2.786
	-0.5	Tensile	621.8	-0.1134	-0.1134	2.739
	0.1	Tensile	637.5	-0.0891	-0.0891	2.743
	0.5	Tensile	787.5	-0.0949	-0.0949	2.819
	0.7	Tensile	995.6	-0.1059	-0.1059	2.935
	0.8	Tensile	985.9	-0.0907	-0.0907	2.937
	0.9	Tensile	760.2	-0.0523	-0.0523	2.838
QQ1 (Axial)	10	Compression	690	-0.0445	-0.0445	2.796
	-2	Compression	698	-0.0600	-0.0600	2.795
	-1	Compression	931	-0.1378	-0.1378	2.902
	-0.5	Tensile	1173	-0.1407	-0.1407	3.012
	0.1	Tensile	1328	-0.1556	-0.1556	3.056
	0.5	Tensile	1359	-0.1313	-0.1313	3.092
QQ1 (Transverse)	10	Compression	239	-0.0434	-0.0434	2.331
	-2	Compression	281	-0.1042	-0.1042	2.399
	-1	Compression	175	-0.1170	-0.1170	2.169
	-0.5	Tensile	166	-0.1087	-0.1087	2.138
	0.1	Tensile	145	-0.0806	-0.0806	2.105
	0.5	Tensile	155	-0.0709	-0.0709	2.138
	0.7	Tensile	141	-0.0480	-0.0480	2.091
P2B (Axial)	10	Compression	1039	-0.0217	-0.0217	2.973
	-2	Compression	1052	-0.0394	-0.0394	2.970
	-1	Compression	1045	-0.0385	-0.0385	2.967
	-0.5	Compression	1043	-0.0239	-0.0239	2.973
	0.1	Tensile	1531	-0.0202	-0.0202	3.145
	0.5	Tensile	1516	-0.0148	-0.0148	3.147
P2B (Transverse)	10	Compression	217	-0.0408	-0.0408	2.308
	-2	Compression	171	-0.0856	-0.0856	2.189
	-1	Tensile	86.6	-0.0717	-0.0717	1.872
	-0.5	Tensile	82.5	-0.0689	-0.0689	1.838
	0.1	Tensile	81.8	-0.0518	-0.0518	1.846
	0.5	Tensile	87.9	-0.0423	-0.0423	1.869
	0.7	Tensile	80.1	-0.0214	-0.0214	1.856
SN5-0291 (Axial)	0.1	Tensile	1185	-0.1157	-0.1187	3.021
WS1	0.1	Tensile	1036	-0.0878	-0.0878	2.555

With their higher fiber elastic modulus, the WindStrand laminates in Figures 8 and 10 show the highest fatigue strengths on a stress basis. The Windstrand laminates showed more influence of damage at the shoulder of the DB specimens (Figure 3) compared with other materials, which could have reduced the static strength and ultimate strain. The carbon based P2B was tested in a rectangular geometry due to this problem. Carbon fiber dominated materials such as P2B are significantly better in tensile fatigue on a stress basis (Figure 10) than any of the glass fiber laminates. Carbon is also competitive with glass laminates on a strain basis at high cycles, shown later.

Constant Life Diagrams

Constant life diagrams, CLD's, have been prepared for materials QQ1 (glass/epoxy) and P2B (hybrid carbon/glass with carbon 0^o plies), in the axial and transverse directions. The full dataset including mean and 95/95 CLD's is available from Wilson's thesis [8], as well as an upcoming Sandia National Laboratories Contractor Report, and only selected results are given. The CLD's are constructed from the model parameters in Table 3. Figure 11 gives a CLD for material DD16 using the same data as Figure 1, but the models defined in this paper (Table 3). Differences between the mean stress CLD's in Figure 11, based on Eq. [1], and in Figure 1, based on the three-parameter model given in Figure 2, are significant only at lifetimes less than 100 cycles, as expected. The dashed lines at 10^7 and 10^8 cycles indicate extrapolation using the fatigue models. Treatment of the time dependent static strength has also been modified in Figure 11 at R = 1.0 to include a time integrated static fatigue model based on 10 Hz frequency [8], which has not yet been applied to other materials.

Figures 12 and 13 give the mean and 95/95 CLD's for the fiberglass/epoxy material QQ1 in the axial direction. As noted above, this material shows poor tensile fatigue resistance compared to other E-glass/epoxy laminates described here, including MD2 and SN5-0291. The transition from compression to tensile failure modes around R = -1 is particularly severe for this material at high cycles, compared with DD16 (Figure 11) or MD2 [2].

Figure 14 compares the mean axial CLD for material QQ1 with that for carbon fiber dominated material P2B on the basis of stress. The carbon is much stronger in both static and fatigue tests. On the basis of strains (Figure 15) the order is reversed for most conditions, except in the tension quadrant at high cycles. Even on a strain basis, however, the carbon fatigue curves are much less steep (Figure 7), and carbon dominated blade designs may be driven by static properties, particularly ultimate compressive strain.

Transverse direction mean stress CLD's for materials QQ1 and P2B are given in Figures 16 and 17. These 0^o dominated laminates are relatively weak in the transverse direction (Table 1) as expected, particularly in tension. (Unlike the axial direction, carbon fibers have a lower elastic modulus than glass in their radial direction, and the transverse ply modulus is typically slightly lower.) The respective CLD's show much better performance in the compressive than the tensile quadrant. Material QQ1, with a higher transverse modulus in the 0^o plies, more ±45's and a small amount of 90^o material in the 0^o fabric, is stiffer and stronger in the transverse direction than the 85% 0^o P2B. However, P2B fails at somewhat higher strains (Table 1), as is typical with the more uniform prepreg laminates.

Spectrum Fatigue Predictions

A comparison for three of the materials, DD16, QQ1, and P2B, was made of their lifetime under the WISPERX wind turbine loads spectrum (rainflow counted [2, 5]) using their respective mean stress CLD's. This is a tensile, single high load dominated spectrum developed in Europe, which has been widely used in spectrum loading studies of blade materials [2, 5, 7]. Based on recent findings for different cumulative damage criteria by Nijssen [2] Miner's sum was used to predict failure, although Sutherland and Mandell [11] have found better predictions with nonlinear models. The required magnification factor for the spectrum in stress or strain was calculated such that failure would occur in a specified number of passes through the spectrum, ranging from 1 to 1000.

Figures 18 and 19 present the results in terms of stress and strain, respectively. Carbon based material P2B is predicted to withstand much higher stress scale factors (and therefore loads) compared to the two E-glass based laminates. On a strain based comparison (which correlates with blade deflection) material P2B shows lower fatigue strains but a much less steep trend, analogous to the S-N trends, compared to the E-glass laminate materials, crossing the QQ1 curve and almost intersecting the DD16 curve by 1000 passes. Comparing the two E-glass based laminates, DD16, with lower fiber content, is superior in terms of strain at all levels (Figure 19) and in terms of stress at higher passes. As noted earlier, QQ1 has a higher elastic modulus compared with DD16, but poorer tensile fatigue resistance. Other E-glass laminates at the higher fiber content of QQ1, such as MD2 and SN5-0291, would be expected to show better results than QQ1, based on Figures 8 and 9.

Conclusions

New fatigue test results have been presented for four materials of current and potential interest for wind turbine blades; these have been compared with two intensively studied materials from existing databases. The new materials represent epoxy resins with 50-61% by volume of three types of fibers, E-glass, WindStrand^{TM} glass, and carbon, as well as differences in E-glass fabric style. A broad range of loading conditions are represented for two of the materials. A number of conclusions can be drawn from these results.

1. The carbon fiber dominated hybrid laminate, P2B, shows major improvements in elastic modulus and static strengths relative to E-glass, but reduced static ultimate strains. Fatigue S-N datasets are uniformly less steep compared with E-glass at all loading conditions. On a stress basis the constant life diagram (CLD) for carbon greatly exceeds that for glass. This is reversed for the strain based CLD except under tensile dominated R-values at high cycles, where P2B exceeds the E-glass based QQ1. Spectrum loading predictions mirror the CLD trends.

2. The WindStrand fiber based laminate, WS1, showed higher elastic modulus, ultimate tensile strength and tensile fatigue resistance on a stress basis, compared with E-glass laminates, but significantly lower compared with the carbon dominated P2B laminate. On a strain basis the fatigue resistance was similar to the best E-glass laminate, SN5-0291, and better than the carbon dominated laminate P2B.

3. Of the E-glass laminates, SN5-0291 with Vectorply E-LT 5500 0^{o}-plies was significantly better in terms of tensile fatigue resistance than other known E-glass laminates. Material QQ1 has relatively poor tensile fatigue resistance, about half the fatigue strength and strain at high cycles compared to SN5-0291. OPTIMAT material MD2 is intermediate between the other two.

4. For the materials in this study, use of a power law fit to the S-N data (Eq.1), combined with a static strength cut-off, provides for accurate mean constant life diagrams above 10^2 cycles. The statistical treatment given here has advantages in apparently requiring less high cycle extrapolation, and can include static data where appropriate. The confidence limits are very close to those based on log cycles [5] for cases explored.

Acknowledgements

This work was funded by Sandia National Laboratories under subcontract Z3609. Prepreg materials were supplied by Newport Adhesives and Composites; Windstrand laminates were supplied by Owens Corning; and SN5-0291 laminates were supplied by Global Energy Concepts through the BSDS program.

References

[1] Mandell, J.F., Samborsky, D.D., and Cairns, D.S. "Fatigue of Composite Materials and Substructures for Wind Turbine Blades," Contractor Report SAND2002-0771, Sandia National Laboratories, Albuquerque, NM, 2002.

[2] Nijssen, RPL. "Fatigue Life Prediction and Strength Degradation of Wind Turbine Rotor Blade Composites," PhD. Thesis, Delft University, the Netherlands, 2006, (ISBN -10190-9021221-3).

[3] Mandell, J.F., and Samborsky, D.D., DOE/MSU Fatigue of Composite Materials Database. 2006 Update. (http://www.sandia.gov/wind/other/973002upd0306.pdf)

[4] Nijssen, R.P.L., "OptiDAT - Fatigue of Wind Turbine Blade Materials Database," 2006, (www.kc-wmc.nl/ optimat_blades).

[5] Sutherland, H.J. and Mandell, J.F., "Optimized Goodman Diagram for the Analysis of Fiberglass Composites Used in Wind Turbine Blades," J. Solar Energy Engineering, 2005, 127:563-569.

[6] Mandell, J.F., and Samborsky, D.D., "DOE/MSU Composite Material Fatigue Database: Test Methods, Materials, and Analysis," Contractor Report SAND97-3002, Sandia National Laboratories, Albuquerque, NM, 1997.

[7] Wahl, N.K., Mandell, J.F., and Samborsky, D.D., "Spectrum Fatigue Lifetime and Residual Strength for Fiberglass Laminates," Contractor Report SAND2002-0546, Sandia National Laboratories, Albuquerque, NM 2002.

[8] Wilson, T.J., "Modeling of In-Plane and Interlaminar Fatigue Behavior of Glass and Carbon Fiber Composite Materials," MS Thesis, Department of Mechanical Engineering, Montana State University, 2006.

[9] Mandell, J.F., Samborsky, D.D., Wahl, N.K., and Sutherland, H.J., "Testing and Analysis of Low Cost Composite Materials Under Spectrum Loading and High Cycle Fatigue Conditions," ICCM-14, SME/ASC, 2003, Paper 1811.

[10] Echtermeyer, A.T., "Fatigue of Glass Reinforced Composites Described by One Standard Fatigue Lifetime Curve," EWEA Conference, 1994, pp. 391-396.

[11] Sutherland, H.J., and Mandell, J.F., "The Effects of Mean Stress on Damage Predictions for Spectral Loading of Fiberglass Composite Coupons, Wind Energy 2005, 8: pp. 93-108.

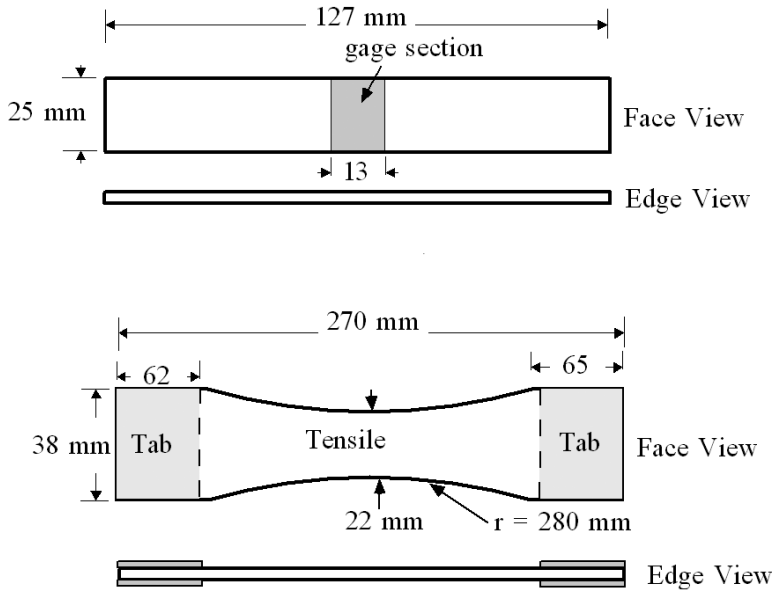

Figure 2. Dog-bone (DB) and Rectangular (Top) Test Geometries.

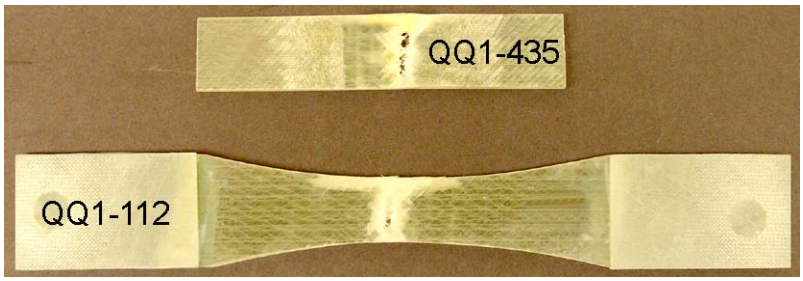

Figure 3. Failed Fatigue Specimens, Showing Grip-Edge Failure for a Rectangular Specimen (Top) and Gage Section Failure for a Dog-bone Specimen.

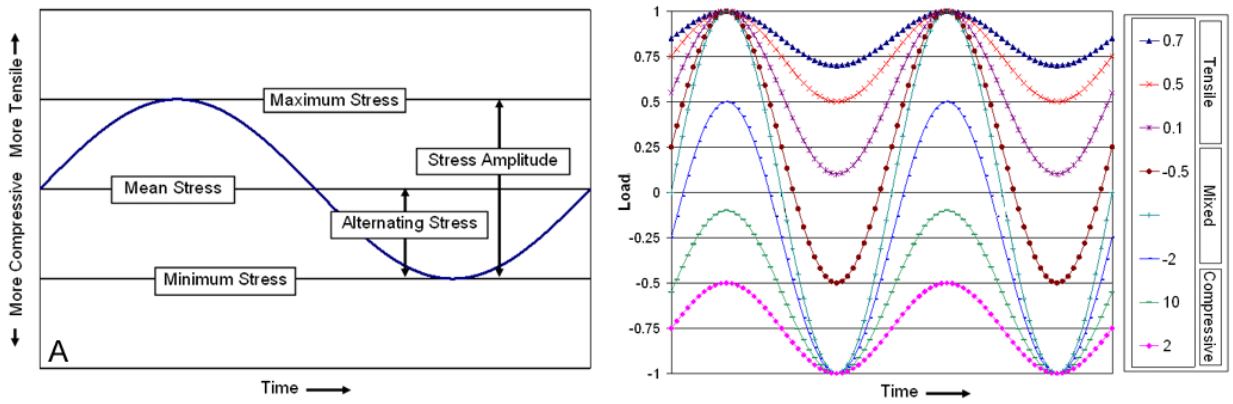

Figure 4. Load Waveforms Showing Definition of Terms (Left) and Illustration of R-values (Right, R = Minimum Stress/Maximum Stress).

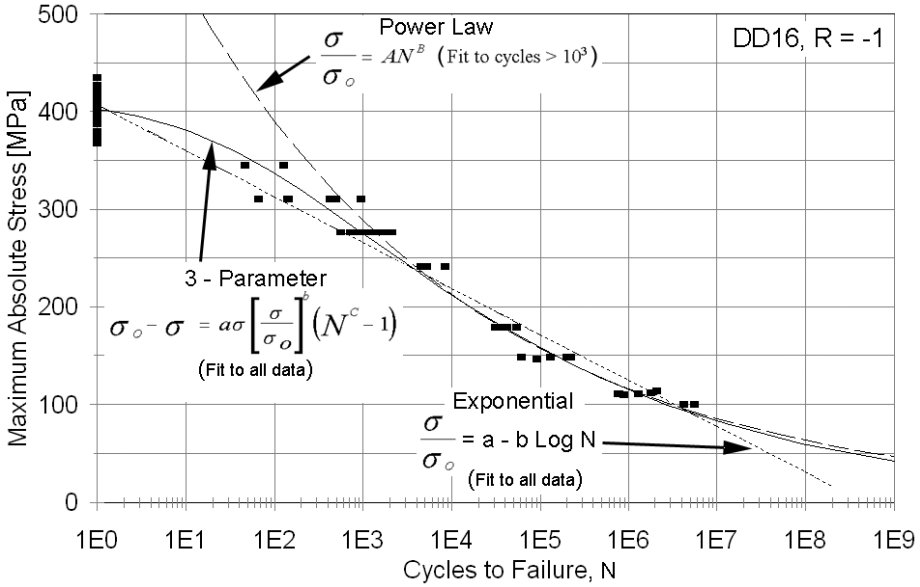

Figure 5. Material DD16 R = -1 S-N dataset with three curve fits, glass/polyester laminate (shown with static compressive strength).

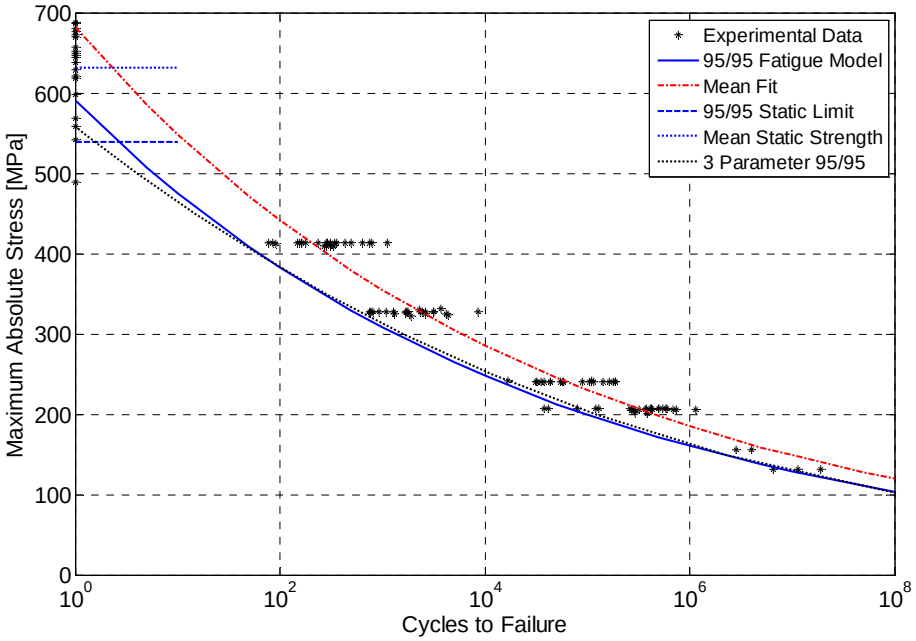

Figure 6. Typical Stress vs. Cycles to Failure Dataset Showing Mean and 95/95 Fits, and 95/95 fit from a log Cycles Model[5], using a Three-Parameter S-N Model, R = 0.1, Material DD16, Axial Direction (Model Fit to All Fatigue Data).

.

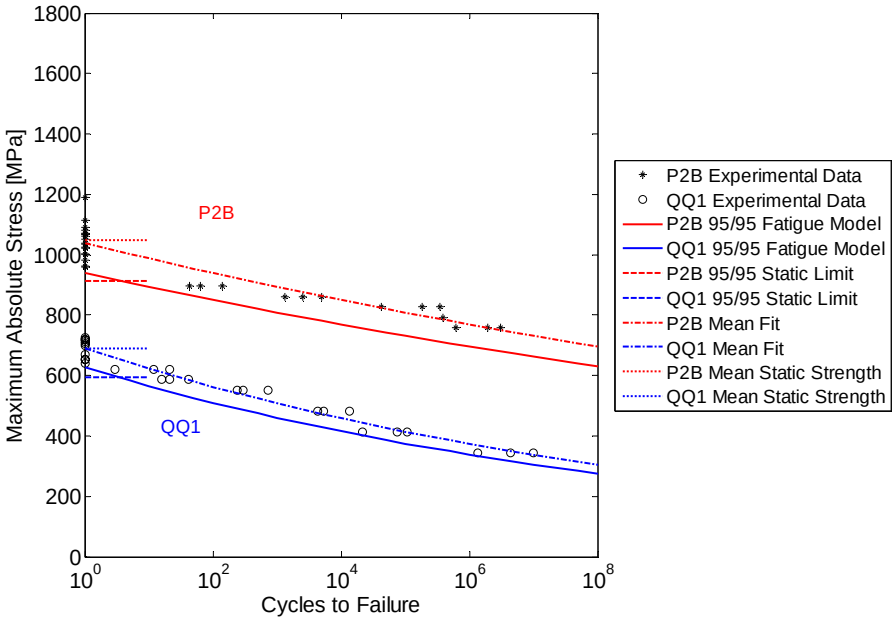

Figure 7(a). R = 10.

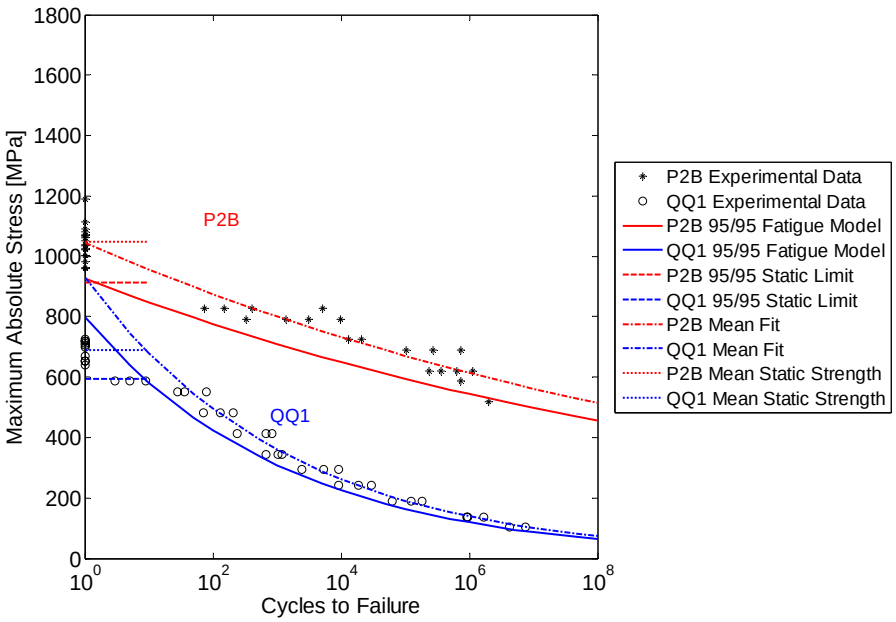

Figure7(b). R = -1.

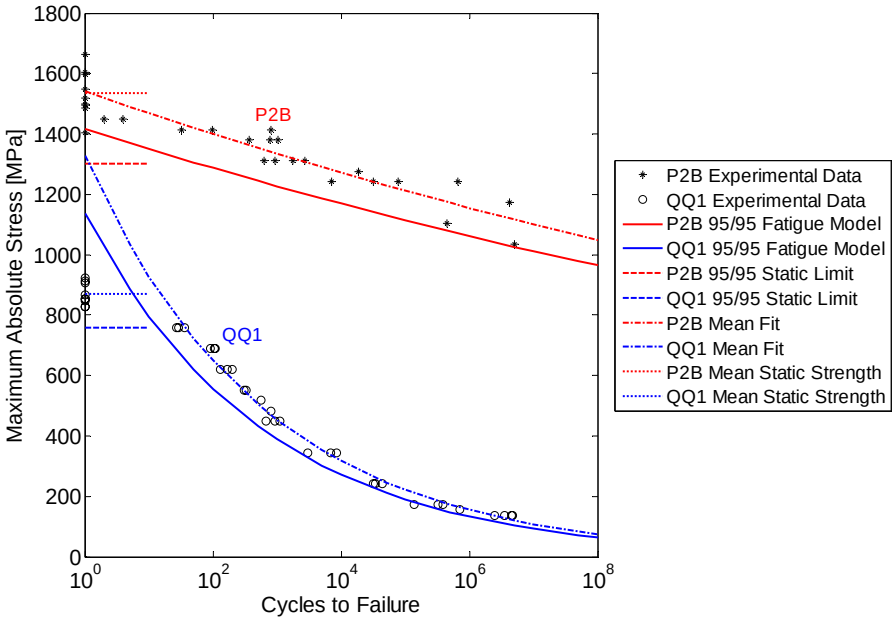

Figure 7(c). R = 0.1.

Figure 7. Comparison of Materials QQ1 (E-glass) with Material P2B (Carbon/E-glass Hybrid) at Three R-Values, Showing Mean and 95/95 Fits.

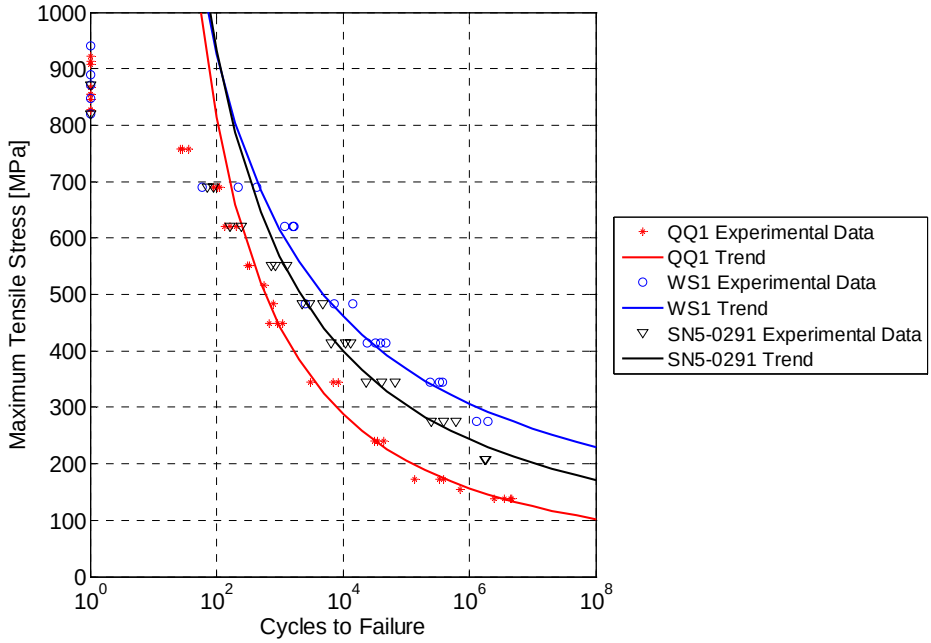

Figure 8. Tensile Fatigue Comparison of E-Glass/Epoxy Materials QQ1 and SN5-0291, and Windstrand/Epoxy Material WS1, R = 0.1, Stress S-N.

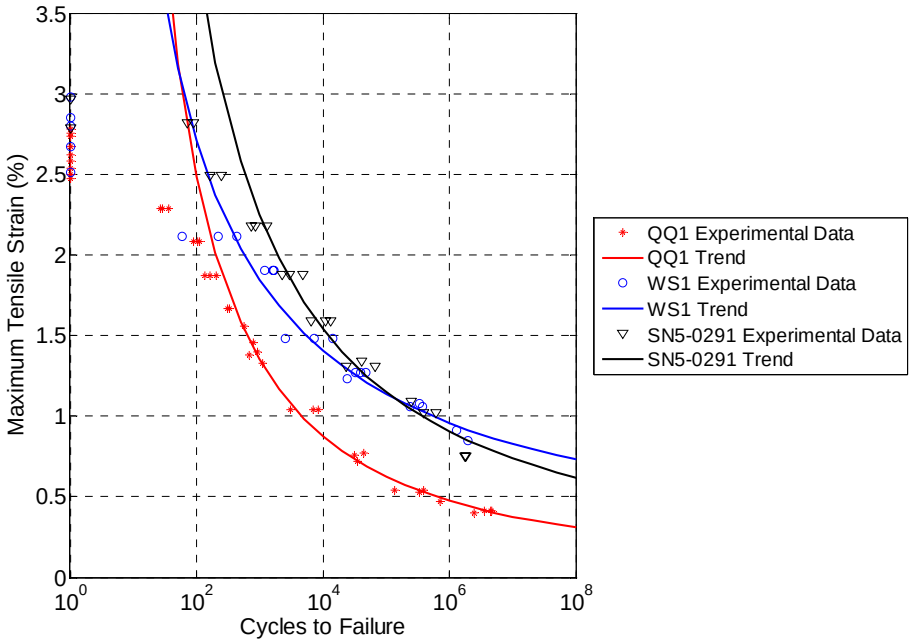

Figure 9. Tensile Fatigue Comparison of E-Glass/Epoxy Materials QQ1 and SN5-0291, and Windstrand/Epoxy Material WS1, R = 0.1, Strain S-N.

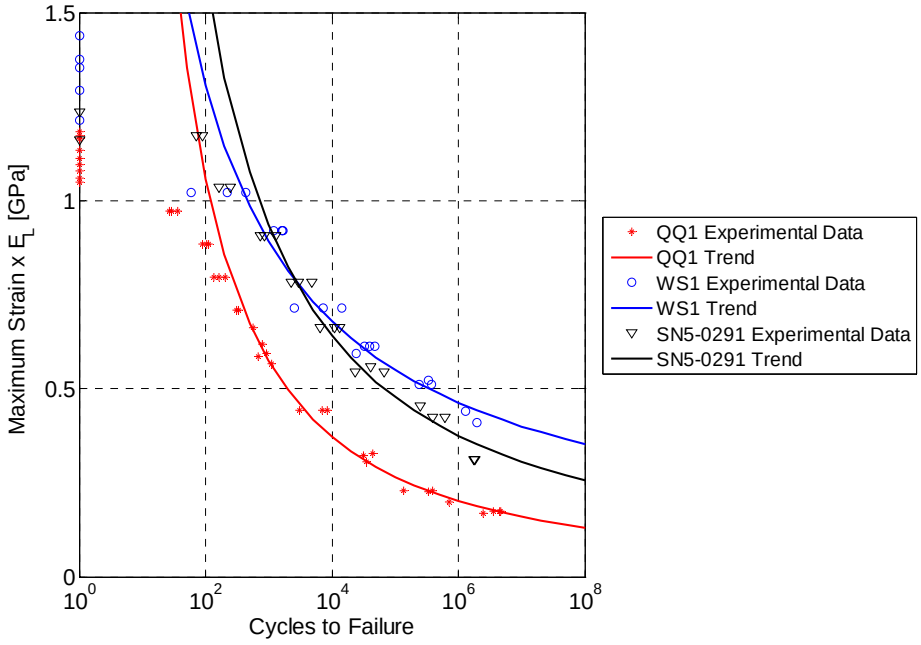

Figure 10. Tensile Fatigue Comparison of E-Glass/Epoxy Materials QQ1 and SN5-0291, and Windstrand/Epoxy Material WS1, R = 0.1, Calculated 0^O Ply Stress (E_L·Strain) vs. Cycles.

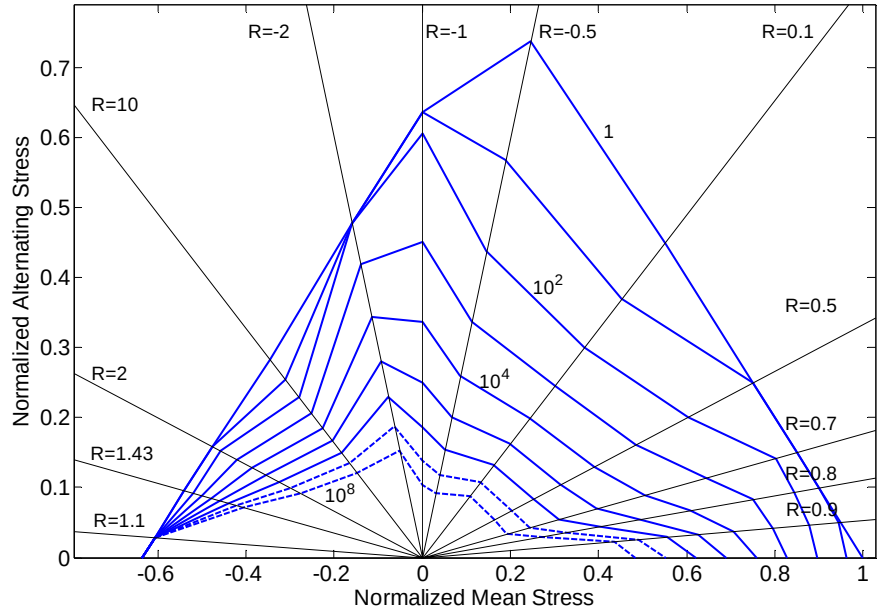

Figure 11. Mean Axial Constant Life Diagram for Material DD16 (Normalized to the Mean Static Tensile Strength).

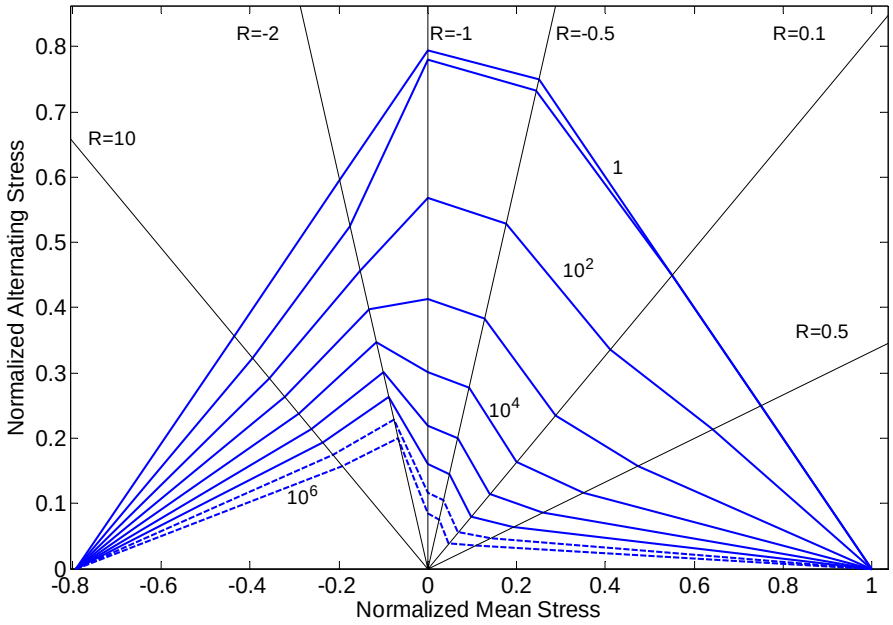

Figure12. Mean Axial Constant Life Diagram for Material QQ1 (Normalized to the Mean Static Tensile Strength).

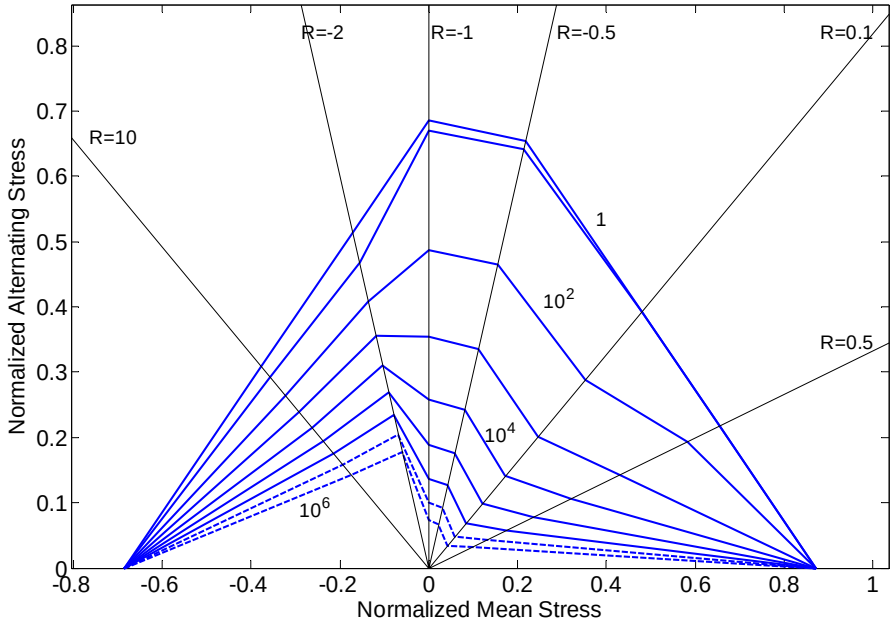

Figure 13. 95/95 Axial Constant Life Diagram for Material QQ1 (Normalized to the Mean Static Tensile Strength).

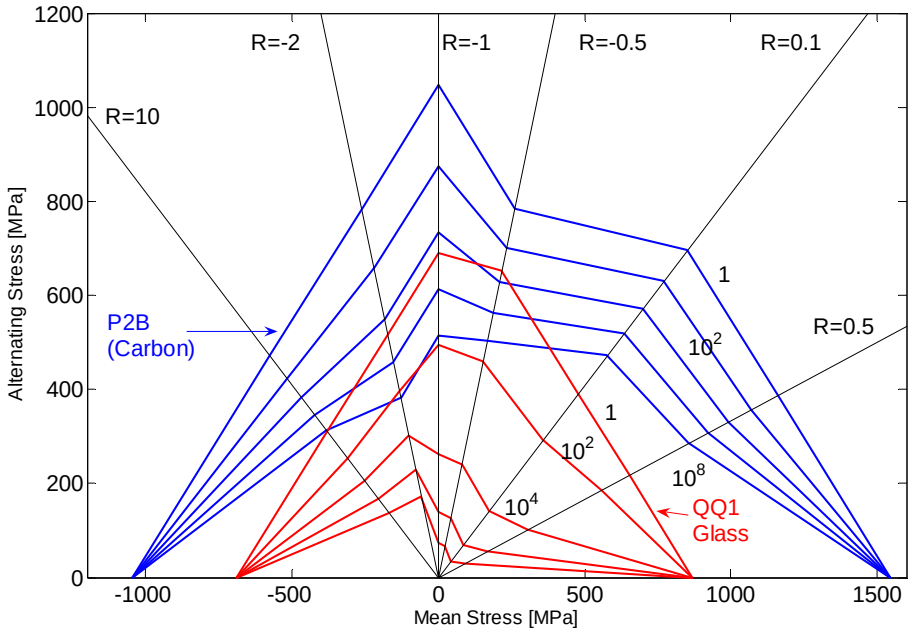

Figure 14. Comparison of Materials QQ1 (E-Glass) and P2B (Carbon Dominated), Axial Direction, Stress Constant Life Diagram, mean stress S-N Model.

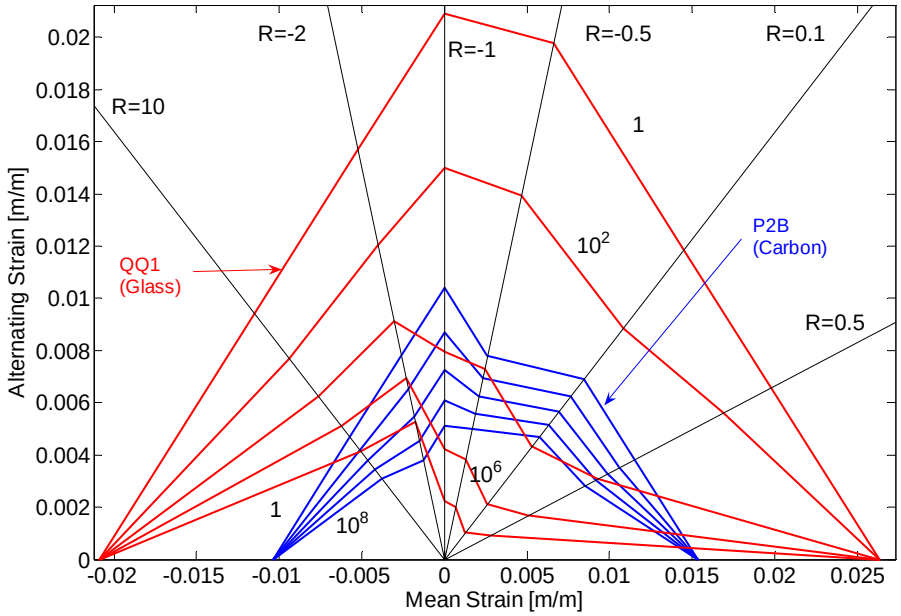

Figure 15. Comparison of Materials QQ1 (E-Glass) and P2B (Carbon Dominated), Strain Constant Life Diagram, Mean Strain S-N Model.

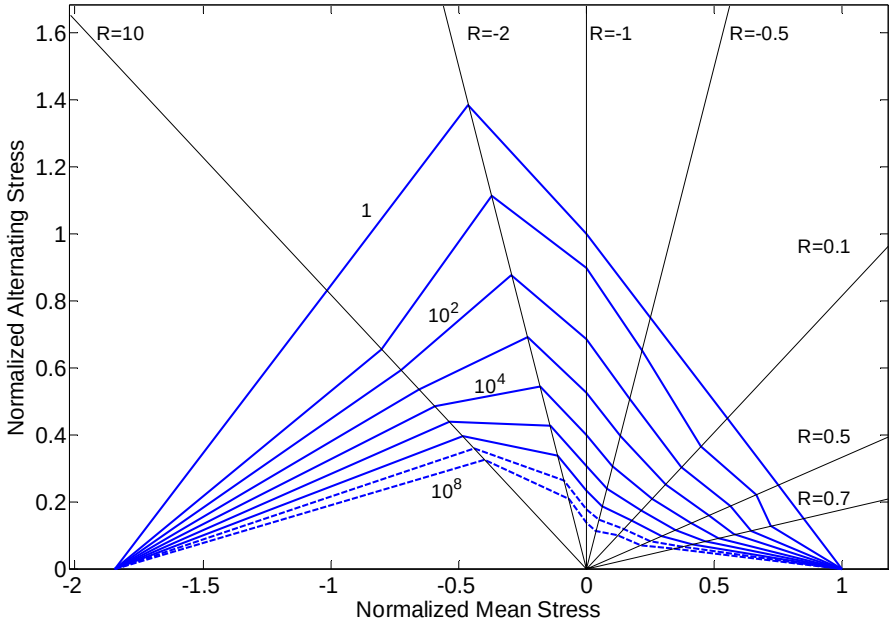

Figure 16. Mean Transverse Constant Life Diagram for Material QQ1T.

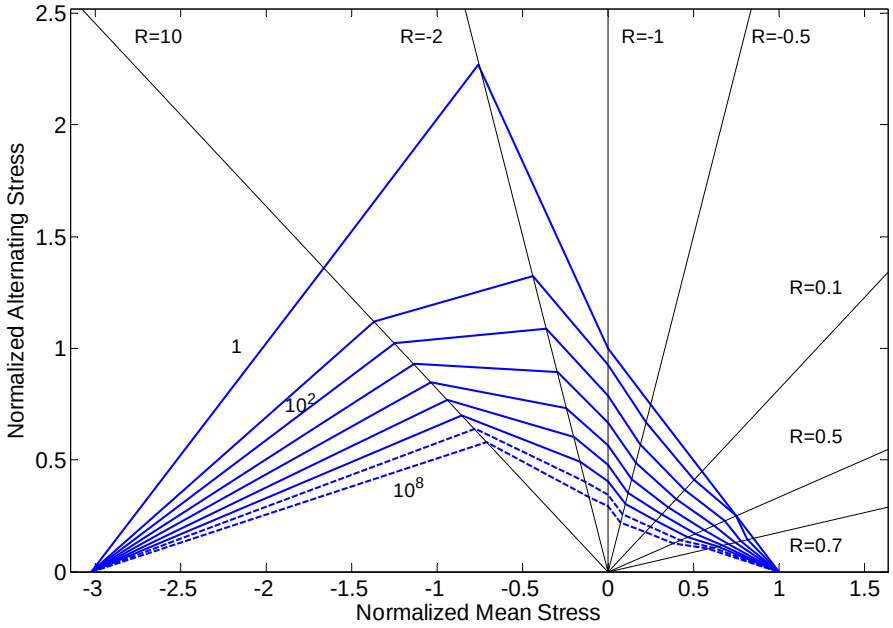

Figure 17. Mean Transverse Constant Life Diagram for Material P2BT.

.

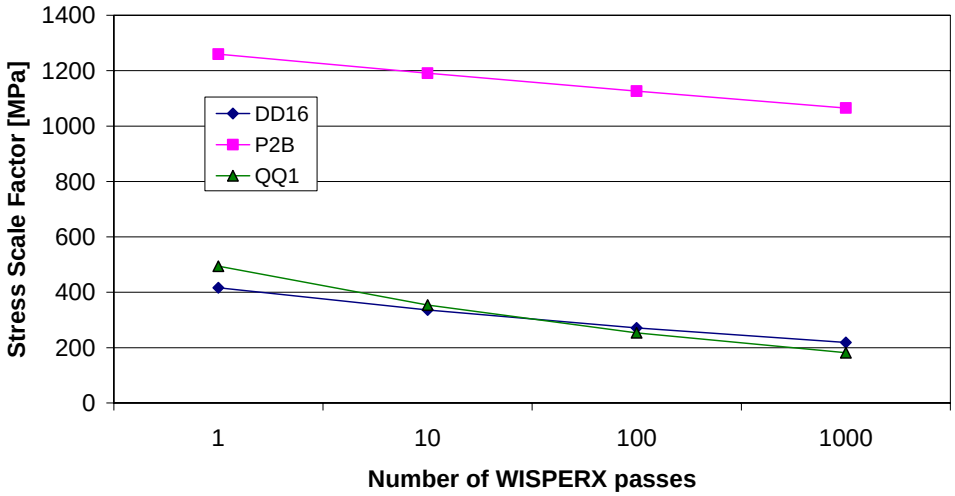

Figure 18. Stress Scale Factors Applied to the WISPERX Spectrum to Achieve a Miner's Sum Equal to 1 (Using the Mean Stress CLD).

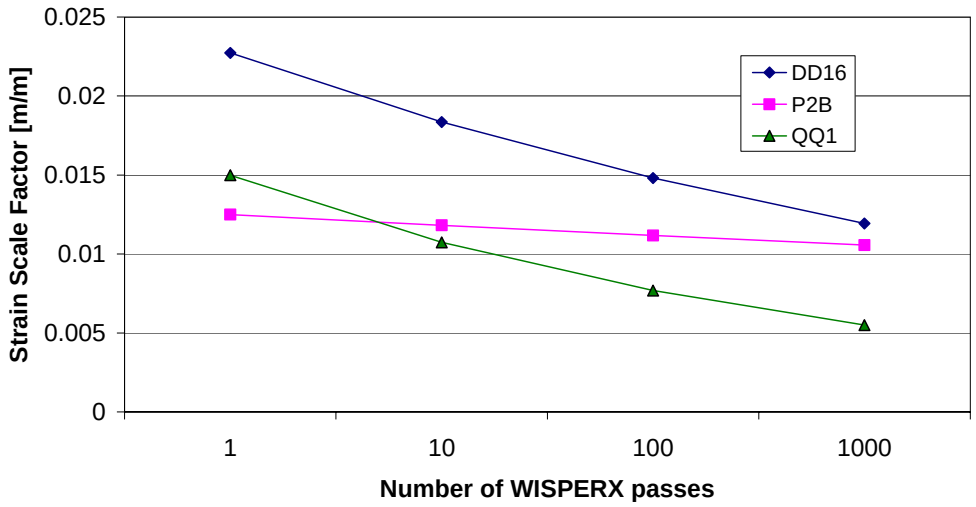

Figure 19. Strain Scale Factors Applied to the WISPERX Spectrum to Achieve a Miner's Sum Equal to 1 (Using the Mean Stress CLD).